Letter

Pre-Steady State Kinetics of Catalytic Intermediates of an [FeFe]-Hydrogenase

Brandon L. Greene, Gerrit J. Schut, Michael W.W. Adams, and R. Brian Dyer

ACS Catal., **Just Accepted Manuscript** • DOI: 10.1021/acscatal.6b03276 • Publication Date (Web): 16 Feb 2017

Pre-Steady State Kinetics of Catalytic Intermediates of an [FeFe]-Hydrogenase

Brandon L. Greene,[†] Gerrit J. Schut,[‡] Michael W. W. Adams[‡] and R. Brian Dyer[†]*

[†] Department of Chemistry, Emory University, Atlanta, Georgia 30322, USA

[‡] Department of Biochemistry and Molecular Biology, University of Georgia, Athens, Georgia 30602, USA

ABSTRACT: [FeFe]-hydrogenases catalyze the reversible production of hydrogen gas from protons and electrons, but the mechanism of catalysis is still the subject of debate. In this report we describe a pre-steady state photo-reduction methodology for correlating putative intermediates to reactivity of an [FeFe]-hydrogenase from *Thermotoga maritima*. In this method, MV^{+} is rapidly formed photo-chemically by pulsed laser excitation and the intermolecular ET and active site dynamics are followed by nanosecond time resolved visible and infrared spectroscopy respectively. The results kinetically validate the H_{ox}, H_{red} and H_{sred} intermediates, strongly supporting a vast body of literature on their involvement in proton reduction.

KEYWORDS: [FeFe] Hydrogenase, Kinetics, Enzymology, Electron Bifurcation, Time Resolved Infrared Spectroscopy

Development of catalysts for the efficient and reversible reduction of protons from water to form H_2, which can be driven by renewable energy sources such as photo-voltaics, has been a significant challenge in the chemical sciences. Microorganisms have developed enzymes called hydrogenases (H_2ases) that catalyze this reaction effectively at the thermodynamic limit, using bioavailable metals nickel and iron, and operate at extremely high kinetic rates.[1-4] These enzymes have been used for photo-catalytic H_2 production by direct coupling to photo-sensitizers,[5-7] or in an integrated bio-reactor, where an electrode supplies H_2 and organisms which contain H_2ases can utilize the electrocatalytically generated H_2 to fix carbon into biomass or other useful fuels.[8-10]

Among the various classes of H_2ases, [FeFe]-H_2ases have been touted as exemplary H_2 production catalysts, due to their rapid proton reduction rates (>1,000 s^{-1}) at very low over-potentials and stronger "bias" towards H_2 production relative to the other major class of H_2ase, the [NiFe]-enzymes.[11-13] Despite their current use in photocatalytic and biotechnological applications,[5,6,14] there are still numerous outstanding questions regarding their catalytic mechanism.[2,15-18] Due in part to the rapid catalysis of these enzymes, mechanistic studies of the [FeFe] H_2ases have relied heavily on steady state spectroscopic techniques to probe the active site electronic structure under various equilibrium conditions[19,20] or electrochemical techniques that lack specificity for the reaction intermediates.[11,21] These studies have resulted in the identification of three distinct active site (H-cluster) configurations of putative intermediates termed H_{ox}, H_{red} and H_{sred} (Scheme 1), which are in equilibrium with reducing equivalents or H_2. Despite the vast body of literature describing the electronic structure of putative H-cluster intermediates, only one study has investigated the kinetics of active site reduction and oxidation,[22] but with insufficient time resolution to kinetically validate intermediates or detect potential new intermediates. Consequently, a major unmet challenge in understanding the mechanism of [FeFe] H_2ases is establishing kinetic competence of the proposed intermediates, as has been established for the [NiFe] H_2ases.[23-25]

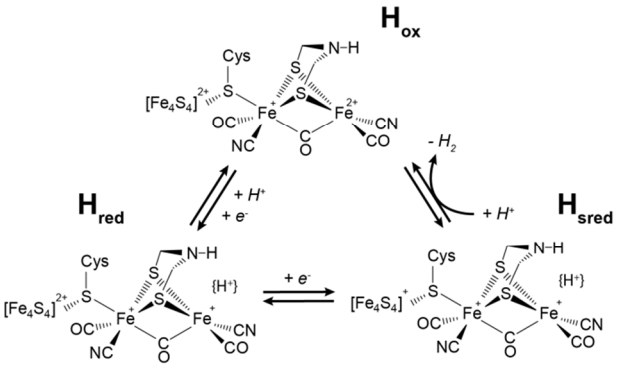

Scheme 1. Proposed H-cluster Intermediates of the [FeFe] H_2ases.

We define kinetically competent active site transformations as those that occur at a rate equal to or exceeding the overall turnover frequency of the enzyme. This task is non-trivial since the turnover frequency (TOF) of most H_2ases is significantly faster than conventional rapid mixing techniques amenable to detailed spectroscopic investigation. One method to address this shortcoming is to couple spectroscopy with sufficient temporal resolution (sub-millisecond) to a rapid photo-chemical reaction initiation mechanism in which a reactant is introduced to the system,[23] or an inhibitor is removed,[26] by a temporally short laser pulse.

In this work we address the kinetic competence of the equilibrium states H_{ox}, H_{red} and H_{sred}, of an electron bifurcating [FeFe]-H_2ase from *Thermotoga maritima* (*Tm*, Supplemental Information Fig. S1). This enzyme simultaneously couples the endergonic oxidation of NADH (E_0' = -320 mV) and the exergonic oxidation of ferredoxin (E_0' = -453 mV) to the reduction of protons to H_2 (E_0' = -420 mV) with an estimated TOF of ~10 s^{-1} at room temperature.[27,28] Using a previously developed rapid photo-reduction method initiated by a short (<10 ns) laser pulse and probing intermolecular electron transfer (ET) and active site dynamics by simultaneous time resolved visible and infrared (IR),[23] we observe rapid enzyme reduction (maximal k_{ET} > 10^7 s^{-1}) and active site chemistry two orders of magnitude faster than the enzyme TOF. The results establish the kinetic competency of the H_{ox}, H_{red} and H_{sred} intermediates, and lay the foundation for new methodology which may be capable of directly resolving elementary steps of proton transfer (PT) and ET involved in H_2 formation analogously to the [NiFe] H_2ases.[23,25]

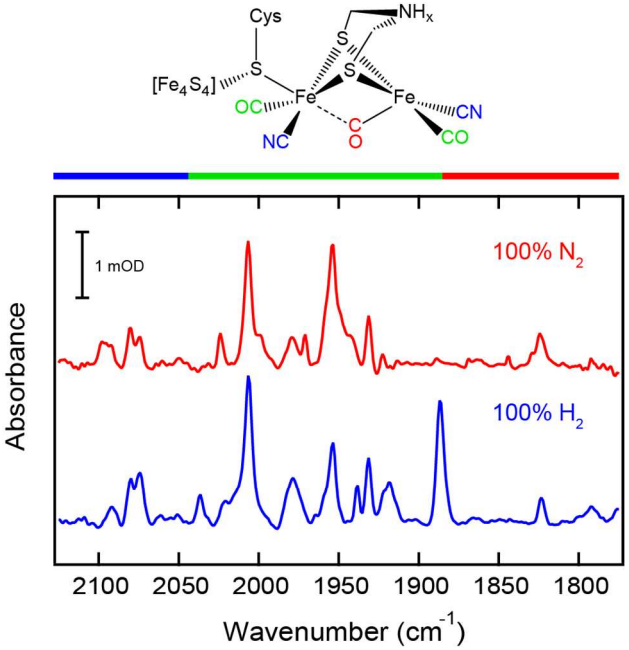

Figure 1. FTIR spectra of the *Tm* [FeFe] H_2ase from the terminal CN to bridging CO region for enzyme prepared under 100% N_2 (red) and 100% H_2 (blue) conditions. The enzyme was concentrated to ~1 mM and loaded into a 50 μm path length CaF_2 FTIR cell. Sample in N_2 was prepared in the presence of 10 mM MV as an indicator of H_2 free conditions, and H_2 sample prepared in presence of 10 mM MV and NADH to mimic photo-reduction experimental conditions.

We initially examined the *Tm* [FeFe] H_2ase prepared as described in the Supplemental Materials and Methods by Fourier transform infrared spectroscopy (FTIR, Fig. 1) to compare the active site of this enzyme to those of other well characterized [FeFe] H_2ases. Under an N_2 atmosphere, numerous peaks were observed between 1800-2150 cm^{-1} in the FTIR spectrum as expected for an active site with CO and CN ligands.[29] From this observation alone, there appears to be no significant differences with respect to other [FeFe]-H_2ases of the H-cluster cofactor of the *Tm* [FeFe] H_2ase, which contains CO and CN ligands, similar to those other of characterized [FeFe]-H_2ases from *Megasphaera elsdenii*,[30] *Desulfovibrio desulfuricans* (*Dd*),[31,32] *D. vulgaris* substrain Hildenborough (*Dv*),[29] *Clostridium pasteurianum* (*Cp*)[33] and *Chlamydomonas reinhardtii (Cr)*.[15,16,34] A detailed and complete assignment of the FTIR spectrum is provided in the Supplementary Discussion and is summarized in Table 1 and Fig. S2. Comparison to other known [FeFe] H_2ases are provided in Table S1.

Table 1. Summary of *Tm* H_2ase intermediate ν_{CO} frequencies.

State	ν_{COt1} (cm^{-1})	ν_{COt2} (cm^{-1})	$\nu_{COb/t}$ (cm^{-1})
H_{ox}	1965	1939	1800
H_{red}	1931	1888*	1793
H_{sred}	1954	1921	1888

* The absorption feature at 1888 cm^{-1} is primarily due to H_{sred}, but may also contain a contribution from H_{red}.

Under H_2 rich conditions states corresponding to H_{ox} (ν_{COt} 1939 and 1965 cm^{-1}), H_{red} (ν_{COt} 1931 cm^{-1}) and H_{sred} (ν_{COt} 1888, 1921 and 1954 cm^{-1}) are observed corresponding to the three active intermediates characterized for other [FeFe]-H_2ases. Further evidence for the presence of H_{sred} is deduced from the rapid loss of this peak upon enzyme auto-oxidation in the IR cell over time (Supplemental Information Fig. S8) and the transient behavior of the resonances associated with this state (*vide infra*). It has been proposed that the H_{sred} state is unstable in the presence of an iron-sulfur (FeS) cluster electron transfer (ET) relay, which will be preferentially reduced,[15,34] therefore the observation of peaks corresponding to H_{sred} in an [FeFe]-H_2ase with ancillary FeS clusters such as that of *Tm* is unexpected. An H_{sred}-like state was previously observed in FTIR spectroelectrochemical titrations of the *Dd* [FeFe]-H_2ase, but the transition between H_{red} and H_{sred} was not reversible.[31] Thus an assignment of a stable steady state H_{sred} is not unprecedented in a multi-FeS cluster containing [FeFe] H_2ase such as that of *Tm* and may suggest a very low oxidation potential FeS cluster proximal to the H cluster. This may be a unique feature of the electron bifurcating [FeFe]-H_2ases, which will require further exploration. The assignment of H_{red} and H_{sred} is therefore well founded within the context of the present work and similarity to other [FeFe] enzymes and is being explored

further to further understand the unique stabilization of the H_{sred} state. In addition to peaks corresponding to H_{ox}, H_{red} and H_{sred}, we observe a population of inactive forms of the H-cluster, termed H_{inact} (ν_{CO} 1980 and 2007 cm^{-1}) and potentially H_{trans} (ν_{COt} 1980 cm^{-1}), suggesting some inactivation under the H_2-free conditions of the experiment. While the observation of inactive species suggests that some oxidation of the enzyme has occurred, this is unlikely to interfere with the pre-steady state kinetic measurements, since this species is not converted to H_{ox}, H_{red} or H_{sred} by incubation with H_2 and MV^+ (Fig. 1). Finally, H_{ox}-CO (ν_{COt} 1963, 1971 and 2009 cm^{-1}) is also observed as identified by the FTIR spectrum collected under 100% CO (Fig. S3) as well as prolonged photolysis studies (Fig. S4).

The presence of a mixture of states spanning the entire characterized redox window of the [FeFe] H_2ases could in principle complicate transient measurements of photo-reduction if any of the species involved are inherently photo-chemically active. H_{ox} is known to be photo-active, cannibalizing the H-cluster and forming H_{ox}-CO.[35] We examined the photochemistry of numerous spectroscopically observable species including H_{inact}, H_{red}, H_{sred} (Fig. S5), H_{ox} and H_{ox}-CO (Fig. S6) under similar excitation fluence as used during photo-reduction experiments. In all cases, no dynamics were observed on the timescales probed (10^{-7} to 10^{0} s). These control experiments suggest that although long timescale illumination can degrade H_{ox}, this process is either too inefficient or too slow to be observed on the timescales of the transient measurements.

Having established a clean photochemical landscape for examining photo-reduction, the *Tm* H_2ase was prepared with methyl viologen (MV^{2+}) and NADPH under N_2 to produce a somewhat oxidized sample for photo-reduction (Fig. S7). NADPH is not a physiological electron carrier for the enzyme (Supplemental Materials and Methods) and thus should be non-interacting. The FTIR spectrum of the as prepared enzyme changed only gradually (Fig. S8) over an extended period of time following transient absorption experiments (*vide infra*), demonstrating little sample degradation over the course of the subsequent experiments. Two photon excitation of the NADPH n→π* transition by UV pulsed laser irradiation (7 ns pulse width at 355 nm) results in rapid (<10 ns) ionization of NADPH, forming solvated electrons and an $NADPH^{+\bullet}$ cation radical.[36-38] Both solvated electrons and the $NADPH^{+\bullet}$ cation radical (as well as the neutral radical) are capable of directly reducing any solvent exposed redox cofactors of the H_2ase, but are short lived forming $H\bullet/H_2$ and NADP dimers respectively on the microsecond timescale. To extend the lifetime of the photo-reduction window, MV^{2+}, a functional *in vitro* redox partner, was used to rapidly capture solvated electrons and $NADP(H)^{\bullet}$ forming MV^+. We have previously demonstrated that this method is capable of generating >100 μM quantities of MV^+ on the nanosecond timescale,[23] creating a rapid chemical potential jump. The net result is a substantial shift from equilibrium, which relaxes to a new redox equilibrium in the presence of a catalyst (*Tm* H_2ase). The photo-generation and subsequent re-oxidation of MV^+ can then be probed by visible transient absorption, sensitive to the MV^+ π→π* transition centered at 603 nm, where there is minimal overlapping absorption from either NADPH, $NADP^+$ or the *Tm* H_2ase. MV^+ formation and decay kinetics were monitored by single wavelength visible transient absorption at 635 nm (Fig. 2).

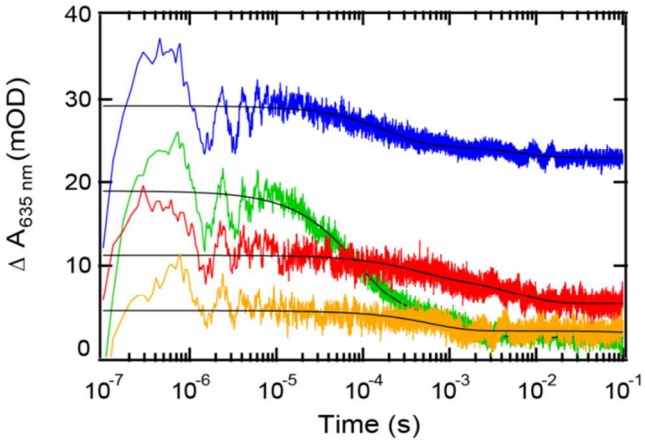

Figure 2. Transient visible kinetics of MV^+ monitored at 635 nm following 355 nm (300 mJ/cm^2) excitation for *Tm* [FeFe] H_2ase sample during 1st (orange) and 5th (red) laser pulse and myoglobin reference during 1st (green) and 5th (blue) laser pulse, including associated biexponential fits (black lines).

A ferric myoglobin sample (metMb, Supplementary Information Fig. S9) was employed as a reference to match the optical density at the pump wavelength (355 nm) to account for the inner filter effect induced by the *Tm* H_2ase FeS clusters, aiding in both transient IR and visible data interpretation. After excitation of the reference metMb solution, a temporally unresolved 19 mOD induced absorbance is observed corresponding to ~360 μM MV^+ (ε_{635} = 6,500 M^{-1} cm^{-1}). The MV^+ then decayed by reaction with metMb with an apparent rate constant of 1.18 (1) x 10^4 s^{-1} (Supplementary Information Fig. S10, Table S2) which consumes all the photo-generated MV^+. We define a single cell exposure as ~50-80 single laser shots rastered over the entirety of the cell such that ~50% of the sample is directly excited (volume of excitation per total volume), followed by equilibration for 30 minutes. After approximately 2-3 pulses over the entirety of the reference cell >90% of the metMb was converted to ferrous deoxymyoglobin (deoxyMb) as indicated by the Soret absorption feature at 436 nm (Supplementary Information Fig. S3). After metMb reduction, the deoxyMb cannot be further reduced by MV^+, which is evidenced by the larger initial MV^+ absorbance (29 mOD) and significant residual absorbance (23 mOD) at 100 ms after pulse 5. Due to the excess NADPH over Mb, the MV^+ generation after complete Mb reduction gives an indication of the total photo-generated reducing equivalents provided by a single laser pulse in this experimental setup. Accounting for the minimal metMb reduction after the fifth pulse (~6 mOD), the total photoproduction of MV^+ could be estimated, yielding 560 μM MV^+. Kinetic analysis of this process at various metMb/deoxyMb equilibria, determined by the number of prior pulses, revealed a consistent trend of decreasing bimolecular metMb reduction kinetics

(Supplementary Information Fig. S10 and Table S2) and increasing initial and residual MV^+ concentration due to less direct metMb reduction by NADP(H)• or solvated electrons.

Photoionization of NADPH in the presence of the *Tm* [FeFe] H_2ase displayed distinct MV^+ generation and decay behavior relative to the Mb reference. Following excitation, an instrument limited rise in MV^+ absorbance was detected which remained constant from 100 ns to 100 µs (Fig. 2, red and orange traces). Very little MV^+ was observed at the earliest times resolved by the experiment, with 5 mOD MV^+ corresponding to ~100 µM MV^+ being formed on this timescale. The photo-generated MV^+ decayed completely with a rate constant of 1.7 x 10^3 s^{-1}, two orders of magnitude faster than the overall enzymatic turnover frequency under similar conditions,[28] and significantly faster than the time resolution of conventional mixing techniques. The difference in initial absorbance of photo-generated MV^+ between the *Tm* H_2ase sample and the Mb reference in the first pulse cannot be ascribed to merely a difference in absorption at the pump wavelength. We thus hypothesize that the enzyme is significantly reduced by solvated electrons or NADP(H)• which is either spectrally (NADPH•) or temporally (e^-_{aq}) unresolved, a phenomenon previously observed in similar work with the [NiFe] H_2ases as well as with the Mb reference.[23]

This is the first kinetics experiment demonstrating that intermolecular ET between MV^+ (or solvated electrons/NADPH•) and an [FeFe]-H_2ase is not rate limiting and leaves a significant temporal window for observing intramolecular ET and active site dynamics following reduction. Upon further pulses, the kinetics became biphasic, with a fast phase (2-7 x 10^3 s^{-1}) and a slow phase (1-2 x 10^2 s^{-1}) (Table S2). The relative amplitude of the fast phase decreased and the slow phase increased as a function of enzyme reduction. The biphasic behavior of MV^+ oxidation has been observed before, albeit indirectly, in the [FeFe]-H_2ase from *Cp*.[39] At this juncture, it is not understood why MV^+ oxidation is biphasic so this will require further study. The total amplitude of the photo-induced MV^+ signal increased and MV^+ oxidation kinetics slowed, again suggesting progressively less direct reduction of the enzyme by solvated electron/NADP(H)• species due to prior reduction. While kinetically non-trivial, the photochemical reduction dynamics of the *Tm* H_2ase clearly demonstrates that the enzyme is reduced on a very rapid timescale, affording ample opportunity to observe pre-steady state dynamics of the H-cluster via the simultaneously collected time resolved IR data.

The active site chemistry of the *Tm* H_2ase was probed by nanosecond time resolved IR spectroscopy simultaneously with visible transient absorption measurements by a collinear dual probe methodology described previously.[23] We selected probe wavenumbers of 1888 ($CO_{t/b}$, H_{sred}/H_{red}), 1931 (CO_t, H_{red}), 1939 (CO_t, H_{ox}) and 1954 cm^{-1} (CO_t, H_{sred}) and examined their kinetics (Fig. 3). In these experiments, it is anticipated that the shift in equilibrium induced by the rapid MV^+ concentration jump will result in reduction of the *Tm* H_2ase, leading to a loss of oxidized species (bleach) and a growth of reduced species (induced absorbance).

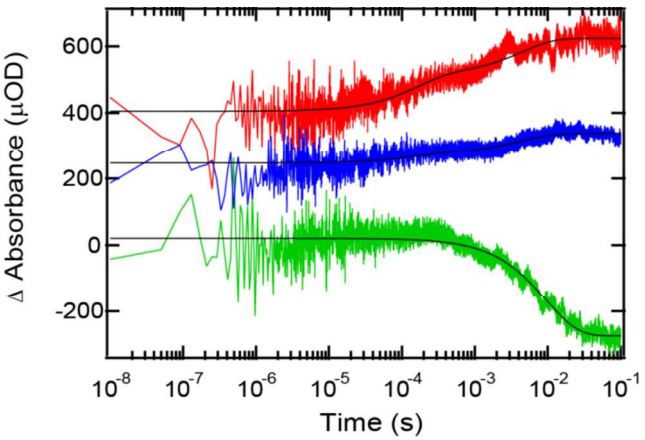

Figure 3. Transient IR traces following a laser induced potential jump (excitation at 355 nm, 300 mJ/cm^2) for H_{ox} (green, 1939 cm^{-1}) and H_{sred} (blue, 1954 cm^{-1}; red, 1888 cm^{-1}) and associated fits (black). A Mb reference transient obtained at the identical frequency is used to subtract the transient solvent heating. Trace offsets added for clarity.

The most intense and spectrally resolved resonance associated with H_{ox} in the ν_{CO_t} region is the absorbance at 1939 cm^{-1}. The kinetics of this species following photo-reduction are shown in green in Figure 3. The transient bleaches with a rate that was well described by a single exponential at 1.04 (1) x 10^2 s^{-1}. This rate is significantly slower than the MV^+ decay kinetics observed in the transient visible experiments suggesting a lag phase in intramolecular ET or PT slowing the active site dynamics relative to intermolecular ET. Despite its slow reduction relative to reduction of the enzyme, the H_{ox} state is still kinetically competent as an intermediate in this [FeFe]-H_2ase. Importantly, no redox activity of H_{inact} or H_{trans} was observed during steady state reduction by MV^+ or H_2, suggesting these species remain silent during the photochemical experiment.

The product of proton-coupled reduction of H_{ox} from steady state measurements is the H_{red} state. To further examine this process we additionally probed the H_{red} state at 1931 cm^{-1}. The transient behavior of H_{red} is anticipated to be complex due to the competing pathways of H_{ox} reduction (which forms H_{red}) and H_{red} reduction (which forms H_{sred}). Indeed this appears to be the case (Fig. S11), with a small induced absorption signature observed with a rate constant of 2.00 (3) x 10^2 s^{-1} when fit to a single exponential, similar to the 1.04 x 10^2 s^{-1} rate constant of H_{ox} decay and indicating a concerted process without buildup of an independent PT or ET intermediate. It also appears by eye that there is an early bleach feature in the transient. When fit to a double exponential, a decay rate of 6.5 (3) x 10^3 s^{-1} and formation rate of 2.20 (5) x 10^2 s^{-1} were determined, but the quality of the fit was only slightly improved from a single exponential fit indicating the S/N was either too low to clearly fit the data or that the transient in fact only represents a single induced absorbance. Both the relative amplitude of the H_{red} transient as well as the slightly faster rate constant of formation relative to H_{ox} decay are consistent with kinetically competitive pathways of H_{red} reduction and H_{ox}

reduction, which becomes evident when examined in the context of the H_{sred} transients. Again, the kinetics of formation and putative decay are kinetically competent for turnover and correlate well with H_{ox}, suggesting this pathway is indeed relevant to catalysis.

The slight bleach feature observed in the H_{red} transient would suggest that H_{sred} is being formed by the photo-reduction process. This was examined at 1888 cm^{-1} (Fig. 3, red) and 1954 cm^{-1} (Fig. 3, blue), which exhibited induced absorption following the MV^+ concentration jump, confirming this conclusion. As noted previously, the absorption feature at 1954 cm^{-1} is unique to H_{sred} among the currently characterized [FeFe]-H_2ases, whereas the peak at 1888 cm^{-1} sits somewhere in between H_{red} (*Cr*, 1891 cm^{-1}) and H_{sred} (*Cr*, 1882 cm^{-1}). Transients at both 1888 and 1954 cm^{-1} displayed induced absorption. The kinetics of formation was bi-exponential in both cases, and fitting of the two independently yielded statistically identical rate constants for both phases. Thus, the two traces were fit globally to a coupled bi-exponential model, yielding excellent agreement with the experimental data and rate constants of 6.3 (3) x 10^3 s^{-1} and 2.20 (4) x 10^2 s^{-1}, both of which were well below the enzyme turnover frequency of 10 s^{-1}. The bi-exponential behavior of these transients is likely a product of the bi-exponential enzyme reduction rate indicating it is limited by enzyme reduction. The relative amplitudes of the absorption features at these two wavelengths were consistent with their steady state ratios and those observed for the H_{sred} state previously[15,17,34] suggesting that the kinetics primarily reflect H_{sred}. Due to the unresolved H_{red} decay, it is unclear whether the $H_{red} \leftrightarrow H_{sred}$ transition is concerted or whether there may be an intermediate. Regardless, it is clear that H_{sred} is also a kinetically competent intermediate of the [FeFe] H_2ases and observed clearly (in the steady state as well as transient measurements) in a H_2ase with ancillary FeS clusters. It is also interesting that the rate of H_{sred} formation (and possibly H_{red} decay) is significantly faster than the rate of reduction of H_{ox}. This could be explained by a slow PT step in formation of H_{red} from H_{ox}, whereas H_{red} reduction occurs by a purely ET mechanism.[15-17,31,34,43] Based on the rapid intermolecular ET, formation of H_{red} from H_{ox} and H_{sred} from H_{red} relative to the overall turnover, it can be reasonably assumed that the rate determining step of proton reduction in this [FeFe] H_2ase is either protonation of H_{sred}, H-H bond formation or H_2 release.

In conclusion, we have examined the steady state FTIR spectrum, pre-steady state intermolecular ET with MV^+ and active site dynamics of the *Tm* [FeFe]-H_2ase over a broad time range, which demonstrate the kinetic competence of proposed intermediates in the catalytic cycle of a bifurcating [FeFe]-H_2ase from *Thermotoga maritima*. The results strongly support the involvement of both H_{ox} and H_{sred} in the catalytic cycle and support the assignment that H_{ox} is reduced in a proton coupled fashion, whereas H_{sred} is formed by ET. This study establishes a basal level of understanding, which will likely be advanced significantly by future measurements of this type capable of directly resolving the elementary steps in proton reduction by these enzymes. In addition, it will be interesting to compare the results presented herein and those to follow, with non-bifurcating enzymes and with biomimetic synthetic analogues of the [FeFe]-H_2ase active site to further understand the reactivity of this unique active site cofactor.[44-49]

ASSOCIATED CONTENT

Supporting Information. Materials and methods, supplemental discussion, schematic representation of the *Tm* [FeFe] H_2ase, FTIR spectra after transient experiments, tabulated CO and CN peak positions of various [FeFe] H_2ases, UV-Vis spectra of the sample and reference, shot dependent visible kinetics traces and rates, and H_{red} transients. This material is available free of charge via the Internet at http://pubs.acs.org.

AUTHOR INFORMATION

Corresponding Author

* Email: briandyer@emory.edu

Author Contributions

The manuscript was written through contributions of all authors. All authors have given approval to the final version of the manuscript.

Funding Sources

This research was supported by the Biological Electron Transfer and Catalysis Energy Frontier Research Center funded by the U.S. Department of Energy, Office of Science, Basic Energy Sciences (DE-SC0012518 to M.W.A.) and by a grant (DMR1409851 to R.B.D.) from the National Science Foundation.

ABBREVIATIONS

H_2ase, hydrogenase; TOF, turnover frequency; Tm, Thermotoga maritima; NADPH, reduced β-nicotinamide adenine dinucleotide phosphate, ET, electron transfer; infrared, IR; PT, proton transfer; FTIR, Fourier transform infrared spectroscopy; Me, Megasphaera elsdenii; Dd, Desulfovibrio desulfuricans; Dv, Desulfovibrio vulgaris substrain Hildenborough; Cp, Clostridium pasteurianum; Cr, Chlamydomonas reinhardtii; MV, methyl viologen.

REFERENCES

(1) Fontecilla-Camps, J. C.; Volbeda, A.; Cavazza, C.; Nicolet, Y. *Chem. Rev.* **2007**, 107, 4273-4303.

(2) Lubitz, W.; Ogata, H.; Rudiger, O.; Reijerse, E. *Chem. Rev.* **2014**, 114, 4081-4148.

(3) Vignais, P. M.; Billoud, B. *Chem. Rev.* **2007**, 107, 4206-4272.

(4) Vincent, K. A.; Parkin, A.; Armstrong, F. A. *Chem. Rev.* **2007**, 107, 4366-4413.

(5) Brown, K. A.; Dayal, S.; Ai, X.; Rumbles, G.; King, P. W. *J. Am. Chem. Soc.* **2010**, 132, 9672-9680.

(6) Brown, K. A.; Wilker, M. B.; Boehm, M.; Dukovic, G.; King, P. W. *J. Am. Chem. Soc.* **2012**, 134, 5627-5636.

(7) Greene, B. L.; Joseph, C. A.; Maroney, M. J.; Dyer, R. B. *J. Am. Chem. Soc.* **2012**, 134, 11108-11111.

(8) Torella, J. P.; Gagliardi, C. J.; Chen, J. S.; Bediako, D. K.; Colon, B.; Way, J. C.; Silver, P. A.; Nocera, D. G. *Proc. Natl. Acad. Sci. U.S.A.* **2015**, 112, 2337-2342.

(9) Liu, C.; Colon, B. C.; Ziesack, M.; Silver, P. A.; Nocera, D. G. *Science* **2016**, 352, 1210-1213.

(10) Nichols, E. M.; Gallagher, J. J.; Liu, C.; Su, Y. D.; Resasco, J.; Yu, Y.; Sun, Y. J.; Yang, P. D.; Chang, M. C. Y.; Chang, C. J. *Proc. Natl. Acad. Sci. U.S.A.* **2015**, 112, 11461-11466.

(11) Parkin, A.; Cavazza, C.; Fontecilla-Camps, J. C.; Armstrong, F. A. *J. Am. Chem. Soc.* **2006**, 128, 16808-16815.

(12) Madden, C.; Vaughn, M. D.; Diez-Perez, I.; Brown, K. A.; King, P. W.; Gust, D.; Moore, A. L.; Moore, T. A. *J. Am. Chem. Soc.* **2012**, 134, 1577-1582.

(13) Hexter, S. V.; Grey, F.; Happe, T.; Climent, V.; Armstrong, F. A. *Proc. Natl. Acad. Sci. U.S.A.* **2012**, 109, 11516-11521.

(14) Ghirardi, M. L.; Dubini, A.; Yu, J.; Maness, P. C. *Chem. Soc. Rev.* **2009**, 38, 52-61.

(15) Adamska, A.; Silakov, A.; Lambertz, C.; Rudiger, O.; Happe, T.; Reijerse, E.; Lubitz, W. *Angew. Chem. Int. Ed.* **2012**, 51, 11458-11462.

(16) Mulder, D. W.; Ratzloff, M. W.; Shepard, E. M.; Byer, A. S.; Noone, S. M.; Peters, J. W.; Broderick, J. B.; King, P. W. *J. Am. Chem. Soc.* **2013**, 135, 6921-6929.

(17) Adamska-Venkatesh, A.; Krawietz, D.; Siebel, J.; Weber, K.; Happe, T.; Reijerse, E.; Lubitz, W. *J. Am. Chem. Soc.* **2014**, 136, 11339-11346.

(18) Mulder, D. W.; Shepard, E. M.; Meuser, J. E.; Joshi, N.; King, P. W.; Posewitz, M. C.; Broderick, J. B.; Peters, J. W. *Structure* **2011**, 19, 1038-1052.

(19) de Lacey, A. L.; Fernandez, V. M.; Rousset, M.; Cammack, R. *Chem. Rev.* **2007**, 107, 4304-4330.

(20) Lubitz, W.; Reijerse, E.; van Gastel, M. *Chem. Rev.* **2007**, 107, 4331-4365.

(21) Baffert, C.; Bertini, L.; Lautier, T.; Greco, C.; Sybirna, K.; Ezanno, P.; Etienne, E.; Soucaille, P.; Bertrand, P.; Bottin, H.; Meynial-Salles, I.; de Gioia, L.; Léger, C. *J. Am. Chem. Soc.* **2011**, 133, 2096-2099.

(22) Erbes, D. L.; Burris, R. H.; Orme-Johnson, W. H. *Proc. Natl. Acad. Sci. U.S.A.* **1975**, 72, 4795-4799.

(23) Greene, B. L.; Wu, C. H.; McTernan, P. M.; Adams, M. W.; Dyer, R. B. *J. Am. Chem. Soc.* **2015**, 137, 4558-4566.

(24) Greene, B. L.; Vansuch, G. E.; Wu, C. H.; Adams, M. W.; Dyer, R. B. *J. Am. Chem. Soc.* **2016**, 138, 13013-13021.

(25) Greene, B. L.; Wu, C. H.; Vansuch, G. E.; Adams, M. W.; Dyer, R. B. *Biochemistry-US* **2016**, 55, 1813-1825.

(26) Mirmohades, M.; Adamska-Venkatesh, A.; Sommer, C.; Reijerse, E.; Lomoth, R.; Lubitz, W.; Hammarström, L. *J. Phys. Chem. Lett.* **2016**, 7, 3290-3293.

(27) Verhagen, M. F. J. M.; O'Rourke, T.; Adams, M. W. W. *BBA-Bioenergetics* **1999**, 1412, 212-229.

(28) Schut, G. J.; Adams, M. W. W. *J. Bacteriol.* **2009**, 191, 4451-4457.

(29) Pierik, A. J.; Hulstein, M.; Hagen, W. R.; Albracht, S. P. J. *Eur. J. Biochem.* **1998**, 258, 572-578.

(30) van der Spek, T. M.; Arendsen, A. F.; Happe, R. P.; Yun, S. Y.; Bagley, K. A.; Stufkens, D. J.; Hagen, W. R.; Albracht, S. P. J. *Eur. J. Biochem.* **1996**, 237, 629-634.

(31) de Lacey, A. L.; Stadler, C.; Cavazza, C.; Hatchikian, E. C.; Fernandez, V. M. *J. Am. Chem. Soc.* **2000**, 122, 11232-11233.

(32) Nicolet, Y.; de Lacey, A. L.; Vernede, X.; Fernandez, V. M.; Hatchikian, E. C.; Fontecilla-Camps, J. C. *J. Am. Chem. Soc.* **2001**, 123, 1596-1601.

(33) Chen, Z. J.; Lemon, B. J.; Huang, S.; Swartz, D. J.; Peters, J. W.; Bagley, K. A. *Biochemistry-US* **2002**, 41, 2036-2043.

(34) Silakov, A.; Kamp, C.; Reijerse, E.; Happe, T.; Lubitz, W. *Biochemistry-US* **2009**, 48, 7780-7786.

(35) Roseboom, W.; de Lacey, A. L.; Fernandez, V. M.; Hatchikian, E. C.; Albracht, S. P. J.; *J. Biol. Inorg. Chem.* **2006**, 11, 102-118.

(36) Lindqvist, L.; Czochralska, B.; Grigorov, I. *Chem. Phys. Lett.* **1985**, 119, 494-498.

(37) Czochralska, B.; Lindqvist, L. *Chem. Phys. Lett.* **1983**, 101, 297-299.

(38) Orii, Y. *Biochemistry-US* **1993**, 32, 11910-11914.

(39) Erbes, D. L.; Burris, R. H. *Biochim. Biophys. Acta* **1978**, 525, 45-54.

(40) Albracht, S. P. J.; Roseboom, W.; Hatchikian, E. C. *J. Biol. Inorg. Chem.* **2006**, 11, 88-101.

(41) Pierik, A. J.; Hagen, W. R.; Redeker, J. S.; Wolbert, R. B. G.; Boersma, M.; Verhagen, M. F. J. M.; Grande, H. J.; Veeger, C.; Mutsaers, P. H. A.; Sands, R. H.; Dunham, W. R. *Eur. J. Biochem.* **1992**, 209, 63-72.

(42) Patil, D. S.; Moura, J. J. G.; He, S. H.; Teixeira, M.; Prickril, B. C.; Dervartanian, D. V.; Peck, H. D.; Legall, J.; Huynh, B. H. *J. Biol. Chem.* **1988**, 263, 18732-18738.

(43) Mulder, D. W.; Ratzloff, M. W.; Bruschi, M.; Greco, C.; Koonce, E.; Peters, J. W.; King, P. W. *J. Am. Chem. Soc.* **2014**, 136, 15394-15402.

(44) Mirmohades, M.; Pullen, S.; Stein, M.; Maji, S.; Ott, S.; Hammarström, L.; Lomoth, R. *J. Am. Chem. Soc.* **2014**, 136, 17366-17369.

(45) Wang, H. Y.; Wang, W. G.; Si, G.; Wang, F.; Tung, C. H.; Wu, L. Z. *Langmuir* **2010**, 26, 9766-9771.

(46) Erdem, O. F.; Schwartz, L.; Stein, M.; Silakov, A.; Kaur-Ghumaan, S.; Huang, P.; Ott, S.; Reijerse, E. J.; Lubitz, W. *Angew. Chem. Int. Ed.* **2011**, 50, 1439-1443.

(47) Tard, C.; Pickett, C. J. *Chem. Rev.* **2009**, 109, 2245-2274.

(48) Camara, J. M.; Rauchfuss, T. B. *Nat. Chem.* **2012**, 4, 26-30.

(49) Hsieh, C. H.; Erdem, O. F.; Harman, S. D.; Singleton, M. L.; Reijerse, E.; Lubitz, W.; Popescu, C. V.; Reibenspies, J. H.; Brothers, S. M.; Hall, M. B.; Darensbourg, M. Y. *J. Am. Chem. Soc.* **2012**, 134, 13089-13102.

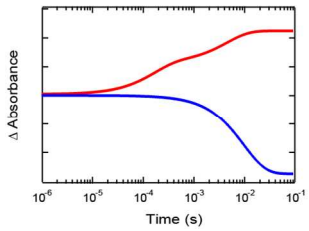
Δ Absorbance
10-6
10-5
10-4
10-3
10-2
10-1
Time (s)

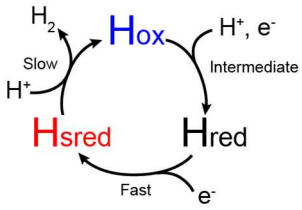
H2
Hox
H+, e-
Slow
Intermediate
H+
Hsred
Hred
Fast
e-